Assessment of Wood and Steel Structures Subjected to Earthquake Mainshock-Aftershock

Yue Li & Ruiqiang Song
Michigan Technological University, Houghton, Michigan, USA

John W. van de Lindt & Negar Nazari
Colorado State University, Fort Collins, Colorado, USA

Nicolas Luco
U.S. Geological Survey, Denver, Colorado, USA

SUMMARY:

This paper works toward a framework to integrate aftershock seismic hazard into Performance-Based Engineering (PBE) through a combination of analytical studies utilizing structural degradation models derived from existing publicly available NEEScentral data. Aftershocks have the potential to cause severe damage to buildings and threaten life safety even when only minor damage is present from the main shock. While aftershocks are normally somewhat smaller in magnitude, their ground motion intensity is not always smaller. Peak ground accelerations (PGA) in aftershock records have been shown to be as high as the PGA in the main shock, and are often of even longer duration and can have different energy content. The earthquake in New Zealand in late 2010 and early 2011 are a perfect example of a much more damaging aftershock due to the location of the aftershock rupture. To date, the description of seismic hazard in PBE has not included the probability of aftershocks. Two approaches to examine the probability of collapse for (1) a steel building damaged from a mainshock; and (2) the reduction in mainshock possible to collapse a building during an aftershock for a light-frame wood building, are investigated as examples.

1. INTRODUCTION

Aftershocks have the potential to cause severe damage to buildings and threaten life safety even when only minor damage is present from the main shock. The Wenchuan earthquake occurred on May 12, 2008 with a magnitude of M7.9. By September 8, 2008, there had been 42,719 total aftershocks, of which 34 were from M5.0 to M5.9, and 8 were from M6.0 to M6.5. An aftershock exceeding M6 was observed on August 5, 2008. These strong aftershocks contributed to the collapse of many of the buildings that sustained damage from the main shock, causing even more loss of life. More than 70,000 people lost their lives in the Wenchuan earthquake and its aftershocks. In addition, the economic loss was estimated to be around $150 billion (RMS 2008, Wen et al. 2009). There have also been occurrences of several large earthquakes, seemingly related but not necessarily aftershocks. For example, consider the series of large earthquakes, known as the New Madrid Earthquakes of 1811-1812 which included three earthquakes between M8.1-M8.3, and caused extensive damage as a result of all three earthquakes. It is often believed that aftershocks are significantly smaller magnitude events than the main shock. While they are normally somewhat smaller this is not always true. The peak ground accelerations (PGA) in aftershock records have been shown to be as high as the PGA in the main shock, but are often of even longer duration (Alliard and Leger 2008) and often have a different energy content. On April 11, 2012, a powerful M8.6 earthquake struck Indonesia, followed by several strong aftershocks with the largest measured M8.2, according to United States Geological Survey (USGS).

This combination of a main shock and aftershock results in the equivalent of a very long duration earthquake, requiring structures to dissipate more energy. PBE has been defined as a seismic

engineering approach based on specific performance objectives and safety goals of building occupants, owners, and the public. It relies on probabilistic or deterministic evaluation of seismic hazard and utilizes quantitative evaluation of design alternatives against the performance objectives.

To date, the description of seismic hazard in PBE has not included the probability of aftershocks. Some preliminary effort has been made to develop a framework to integrate aftershocks into PBE. Yeo and Cornell (2005) proposed a conceptual analytic framework for the incorporation of aftershocks into performance-based earthquake engineering. They pointed out that "the investigation of aftershock on performance-based earthquake engineering is still in its infancy at every stage". Clearly there is significant uncertainty in the capacity of damaged buildings after main shocks and the characteristics of aftershocks are quite complex. Thus, a systematic methodology to integrate main shock-aftershock seismic hazard into PBE would be needed.

In this paper, two approaches to investigate the effect of mainshock-aftershock sequences are discussed using accurately calibrated numerical models for degraded and damaged buildings as examples. One approach is to investigate the probability of collapse for a steel building damaged from a mainshock. Another approach is to consider the reduction in mainshock possible to collapse a building during an aftershock for a light-frame wood building. The publicly available testing data at Network for Earthquake Engineering Simulation Research (NEESR) data repository NEEScentral provides an opportunity to calibrate damage models and evaluate building performance when subjected to multiple earthquakes. It is very common to perform multiple tests on a specimen, with one or more on an already damaged structure, making these data sets perfect for inclusion in the proposed study. Two data sets, a steel moment-resisting frame building and an engineered light-frame wood building, at NEESR are used to calibrate damage models for analysis in the main shock – aftershock sequences.

2. PROTOTYPE STEEL AND WOOD STRUCTURES AND CALIBRATION

The prototype 4-story steel moment-resisting frame structure in East-West (E-S) direction is shown in Fig. 1. Two 1:8 scale model frames were built and tested until collapse at NEESR facility at the State University of New York at Buffalo. Details of the model and tests can be found in Lignos et al. (2011).
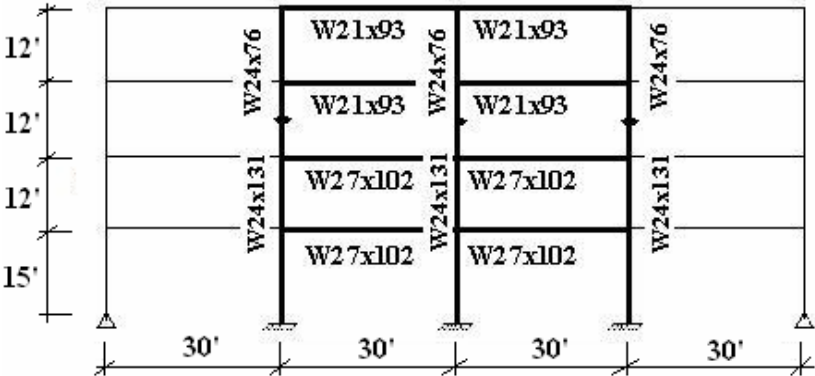
Figure 1. A four-story moment-resisting prototype building in EW direction

The steel moment-resisting frame structure is modelled with elastic beam-column element connected by the zerolength element, served as the plastic hinge rotational spring to represent the structural nonlinear behaviour, using OpenSees (2012). The bilinear hysteretic response of the spring is based on the Modified Ibarra Krawinkler Deterioration Model (Lignos et al. 2009). In order to simulate P-Delta effects, a leaning column carrying gravity loads is linked to the frame and modelled as beam-column elements jointed by zeroLength rotational spring elements with very small stiffness values to avoid carry significant moments. Since each flexural member is modelled as an elastic element with plastic hinge rotational springs at the end, the structural properties of these component must be modified so that the equivalent structural properties of the assembly is the same as the actual frame members

(Ibarra and Krawinkler 2005). To calibrate the finite element (FE) model of prototype steel frame in EW direction, the first three modal periods, pushover and fragility curves are compared from the FE model and the values given in Lignos et al. (2009).

Figure 2 shows a photo of a two-story woodframe townhouse that was tested as part of the NSF-funded NEESWood project at the NEES@Buffalo equipment site producing a landmark data publically available data set. There were five test levels ranging from a test of just the woodframe with no drywall or stucco finishes to the completed building with all finishes and furniture. The completed building data set was used in the modelling and aftershock collapse procedure described here. Specifically, a hysteretic model was fit to the global hysteresis generated during an MCE level tri-axial shake. This Single Degree-of-Freedom (SDOF) model intrinsically accounted for sliding of the sill plate, splitting of the plate, uplift, and shear deformation, but there are plans to extend it to a more complex model in the near future.

Figure 2. NEESWood benchmark test structure

3. MAINSHOCK-AFTERSHOCK GROUND MOTIONS

Structural performance during an earthquake is impacted by uncertainties in both seismic loading and structural resistance. The selection of ground motion records to represent realistic amplitude, frequency content, and duration for aftershocks is a challenge, in part because disaggregation of seismic hazard due to main shocks and aftershocks are typically different. The magnitude distribution of aftershocks is independent of elapsed time after the mainshock, which means large aftershocks may occur several months later, as observed after the Wenchuan Earthquake. Meanwhile, the mean occurrence rate and the distribution of aftershocks have strong correlations with mainshock magnitude (Reasenberg and Jones 1994; Yeo and Cornell, 2005).

A suite of 22 ground motions (ATC 2009) assumed to be mainshocks were examined for the steel and wood frame building models using a multi-record IDA. The magnitude for each of the ground motions is between M6.5 to M7.6. The combination of mainshock and one aftershock for the steel structure is firstly considered. To simply the relationship between mainshock and aftershock, the frequency contents and durations are assumed to be the same for both the mainshock and aftershock. In order to examine the effects of a certain level of structural damage sustained from mainshock followed by an aftershock on the structural collapse capacity, the intensity level of mainshock is scaled by multiplying the factor $\gamma_{m,a}$ in the equation (3.1) to obtain the specific structural damage condition. The factor D_m which represents damage level of structure to mainshock, can be determined in the IDA curve of building subject to mainshock. The damage levels of building in the current methodology are defined by the peak transient drifts. According to the relevant definition of damage levels (e.g. ASCE 41), the transient drift value can be determined and then the corresponding spectral acceleration (S_a) will be

found in the IDA curve. Then a relationship between the specific structural damage level and the corresponding S_a is created. Based on the earthquake ground motion scaling rules in the equation (3.1), the effect of different structural damage states from mainshock on structural responses can be determined by combining the specified intensity level of mainshock and aftershock.

$$\gamma_{m,a} = \gamma_m \times \gamma_a \, ; \qquad\qquad\qquad\qquad\qquad\qquad (3.1)$$

$$\gamma_m = \frac{D_m}{S_{a,m}} \, ; \quad \gamma_a = \frac{S_{a,a}}{SF}$$

where

$\gamma_{m,a}$: Scaling factor for mainshock in mainshock-aftershock sequences;

γ_m, and γ_a : Scaling factor for mainshock and aftershock, respectively;

D_m : Damage level factor of the structure due to mainshock;

$S_{a,m}$, and $S_{a,a}$: S_a of mainshock and aftershock at the fundamental period of structure, respectively;

SF : Scaling factor for intensity level of the aftershock.

In the wood structure model, for each IDA a set of basic rules provided a means to select a collapse S_a range and a corresponding collapse drift range. Rank ordering these seismic intensity ranges (and their corresponding collapse drift ranges) for each of the 22 records provides a collapse band. This band represents the probabilistic range of collapse at a range of seismic intensities. The seismic intensity corresponding to collapse is denoted by $S_{a_m}^i$ and $S_{a_m}^j$, for the mainshocks and aftershocks and $i=1, ..., 22$ represents the earthquake record number used. The index m indicates mainshock. The collapse drift is denoted by Δ_*^i and Δ_*^j is associated with $S_{a_{m,*}}^i$ and $S_{a_{m,*}}^j$ values.

Of interest here is the earthquake intensity that can occur in the mainshock such that an aftershock of known intensity barely results in collapse during the aftershock. This reduction factor can be applied to mainshocks, a new seismic intensity calculated, and the change in collapse risk quantified. So, a mainshock-aftershock combination is constructed by scaling the mainshock and aftershock to $cS_{a_{m,*}}^i$, where c is a constant value which is taken to be 0.8 in this paper. Next IDA analysis is run by using the mainshock-aftershock records. The new $S_{a_{m-a}}^{i-j}$ (where the index indicates the combined mainshock-aftershock record), is tied to the value of Δ_*^j determined in the previous analysis. The parameter Ψ is introduced to be multiplied by the c value to rescale the mainshock to the value of $c\Psi$. The value of this parameter is determined as:

$$\Psi = \frac{S_{a_{m-a}}^{i-j}}{S_{a_m}^j} \qquad\qquad\qquad\qquad\qquad\qquad (3.2)$$

This reduction in the seismic intensity needed to collapse a building if an aftershock of known intensity occurs is thus determined.

4. INCREMENTAL DYNAMICS ANALYSIS FOR COLLAPSE CAPACITY

The seismic capacity of a structural system can be determined by incremental dynamic analyses (IDA) (Vamvatsikos and Cornell 2002). An IDA involves a series of Nonlinear Dynamics Time History Analysis of the structure subjected to an ensemble of ground motion records, each record in the ensemble being scaled to multiple levels of intensity with respect to the S_a at the fundamental period of the structure. The resulting family of curves describes the structural response (measured by

maximum drift) versus earthquake intensity (measured by S_a). Fig. 3 shows the IDAs for the steel structure that only considers the 22 ground motions as mainshock, while Fig. 4 demonstrates the mean IDA curve.
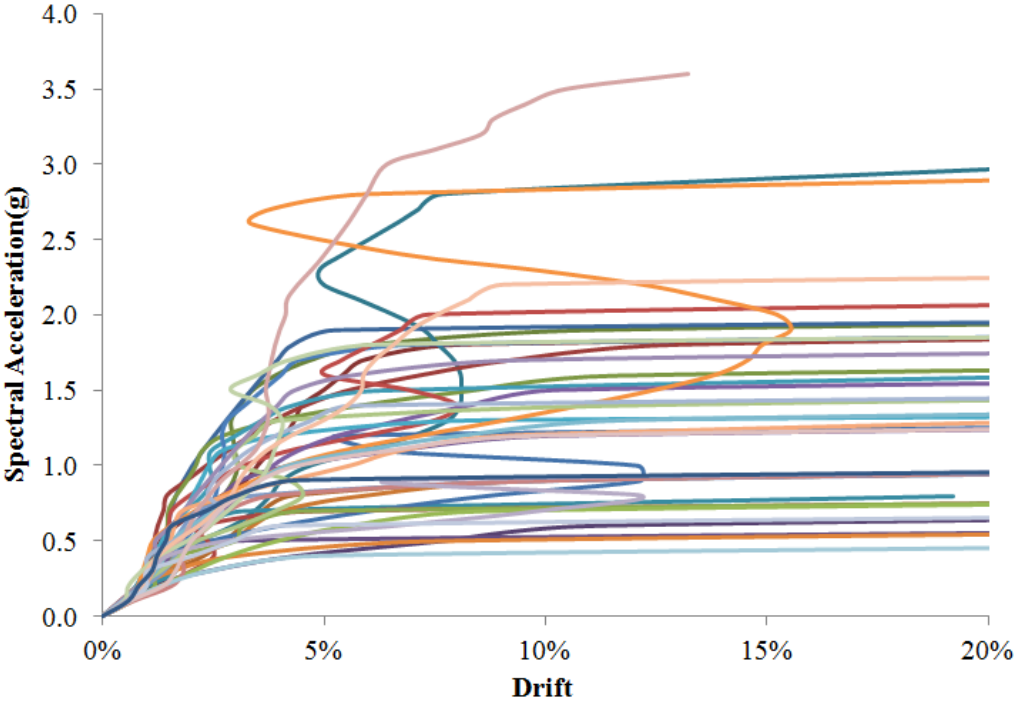

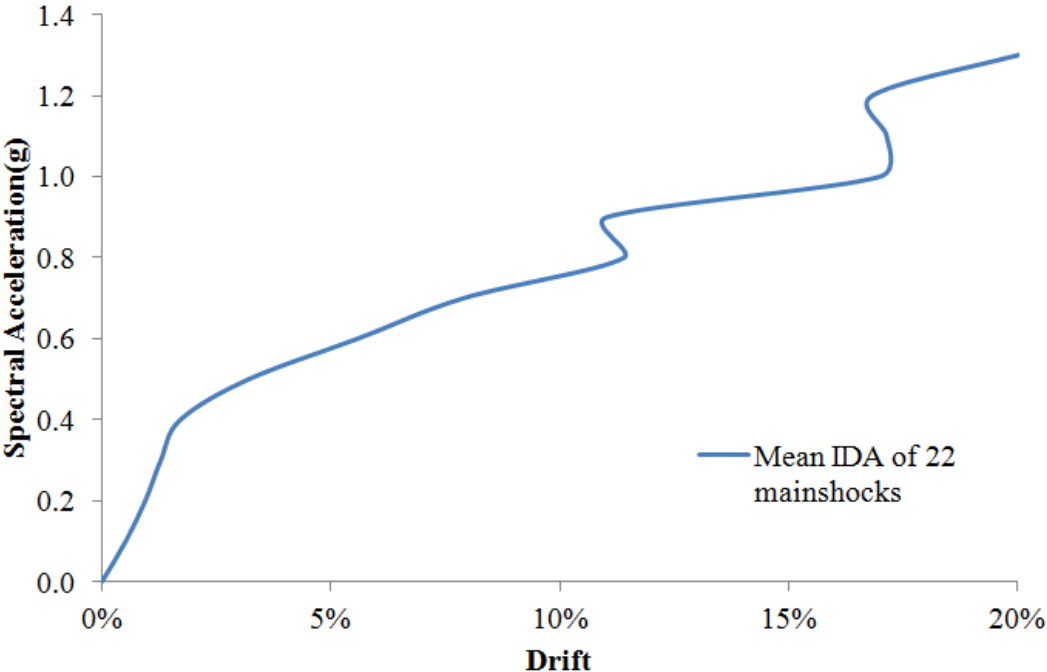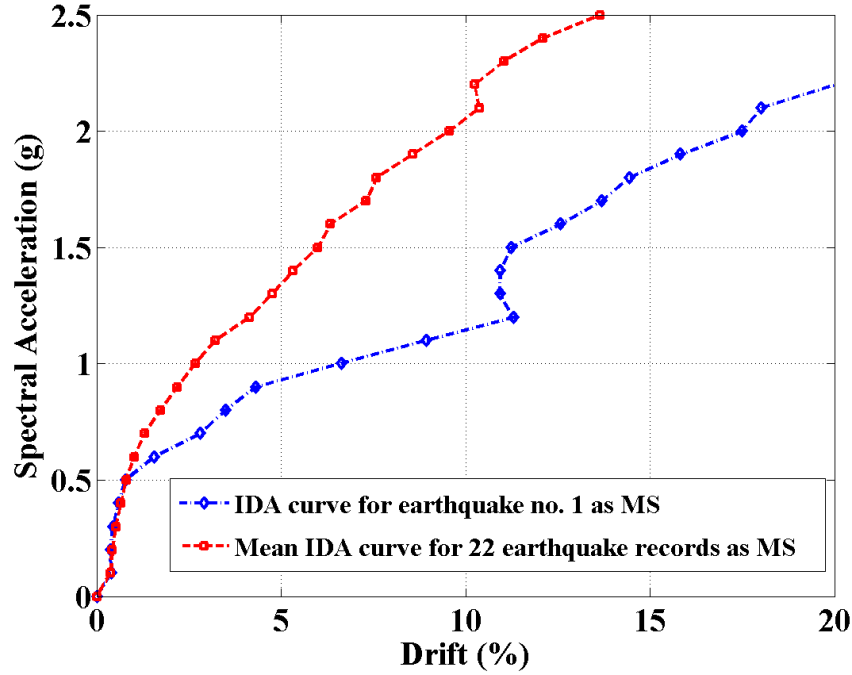**Figure 3.** IDA curve for steel structure subjected to mainshock

Figure 4. Mean IDA curve for steel structure subjected to mainshock

Fig. 5 presents an IDA in terms of drift for earthquake number 1 as mainshock and then the mean value of all 22 IDA's to show the scatter which is typical of IDA's. Table 1 shows the corresponding collapse drifts assigned to each of the earthquake records via inspection of the IDA results. For earthquake number 1 this is 7.8% drift which one can see corresponds to the average of the flattening portion of the IDA.

Figure 5. IDA curve for wood structure subjected to mainshock.
(Note: All IDA curves are not shown for clarity)

Table 1 presents the collapse seismic intensities and the associated collapse drift which is determined on the basis of assuming collapse as 20% slope in the IDA curve. However, the average value for the collapse band is utilized.

Table 1. The collapse seismic intensities and the associated collapse drifts

Earthquake record No.	$S_{a_{m,*}}^{i}$ (g)	Δ_{*}^{i} (%)
1	1.05	7.8
2	1.15	6.1
16	1.35	4.5
8	1.45	14.0
6	1.65	2.6
11	1.65	14.7
13	1.65	6.6
5	1.8	13.0
19	1.8	14.1
14	1.95	4.7
18	1.95	10.9
7	2.05	10.2
9	2.05	9.8
12	2.05	10.5
17	2.15	6.6
15	2.25	6.3
21	2.25	10.1
3	2.35	8.5
4	2.45	13.1
20	2.5	8.2
22	2.5	3.9
10	2.5	4.0

As an example, consider earthquake number 1 and the addition of four random aftershocks selected from the same suite and combined to form the mainshock-aftershock train using the procedure described earlier.

Table below contains the Ψ values which are defined in section 3, and are calculated for earthquake 1 combining it with earthquake records 1, 10, 14 and 19 as aftershocks. Of interest is the significant reduction in the mainshock intensity needed to collapse the building if an aftershock having a seismic intensity of 80% of the mainshock occurs. By determining the correlation between the aftershock scaling constant, c, and the mainshock reduction factor Ψ, it may be possible to determine the change in seismic hazard as a function of c.

Table 2. Ψ values associated with MS-AS combination

MS-AS	Ψ values
1-1	0.85
1-10	0.37
1-14	0.47
1-19	0.66

## 5. COLLAPSE FRAGILITY FOR UNDAMAGED AND DAMAGED BUILDINGS

A fragility is the probability of a limit state (e.g. incipient collapse) being exceeded, conditioned on some intensity measure – most often the S_a at the fundamental period of the structure. A multi-record IDA involves a series of nonlinear time history analyses of the structure subjected to an ensemble of ground motion records, each record in the ensemble being scaled upward to multiple levels of intensity with respect to the S_a at the fundamental period of the structure. The resulting family of curves describes the structural response (measured by maximum drift or energy dissipated) vs. earthquake intensity (measured by S_a). From the calibrated models, fragilities were developed for structures under varying levels of degradation or damage.

Based on the IDA curves for the steel structure, the structrual collapse capacity is determined as the last point on the IDA curve that is large than the inital 20% tangent slope of the curve (Vamvatsikos and Cornell 2002). Treating the collpase capacity in terms of S_a as a random sample, a lognormal dirstibution is fitted to generate the collapse fragility curve, which is shown in Fig. 8. The median and the logarithmic standard deviation of the collapse capacity of the undamaged building model are 1.16g and 0.51, respectively.

According to the ASCE-41 (2006), the strucutral performace for steel moment frames can be defined as three levels: immediate occupany, life safety, and collapse prevention, defined by 0.7%, 2.5%, and 5% transient drift, respectively. The three performance levels can be viewed as minor, moderate, and severe damage. In order to investigate the effect of various levels of damage from mainshock on the structural collapse capacity, the IDA are carried out for steel structure subjected to different levels of mainshock-aftershock sequences (shown in Fig. 7). Fig. 8 compares the collapse fragility curves for the damaged building at three damage levels. For example, the fragility curve of mainshock(0.7%) + Aftershock represents the probability of collapse for the building that was minorly damaged building in the mainshock, i.e. 0.7% drift.. The collapse fragility curve for the building that substains minor damage almost overlaps the fragility curves of the undamaged building. However, there is obvious difference between the collapse fragility curves between the moderately or severely damaged building and the undamaged building.
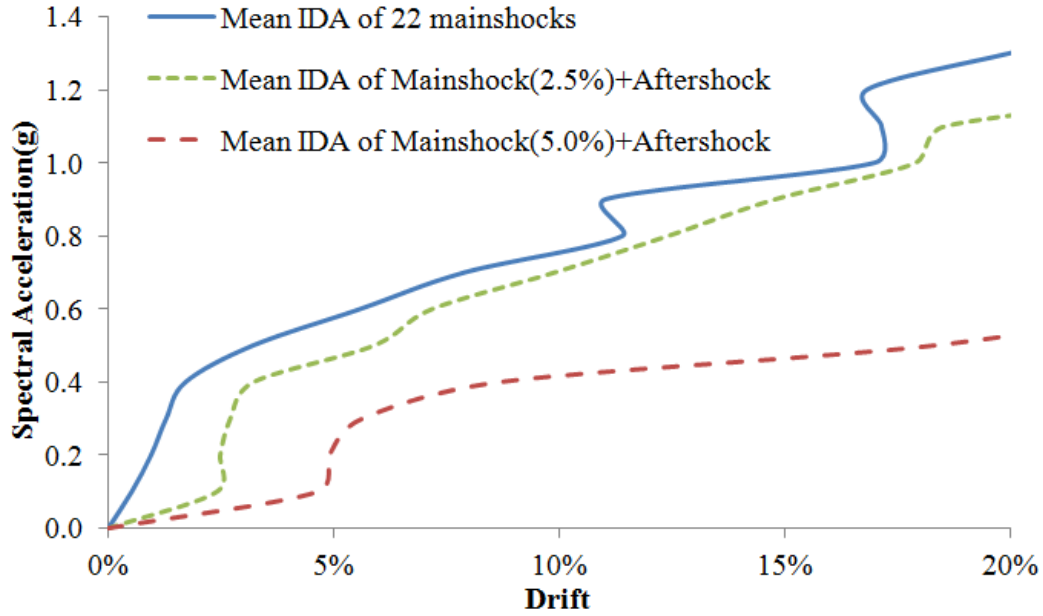
Figure 7. Mean IDA curve for steel structure subjected to different levels of mainshock-aftershock sequences
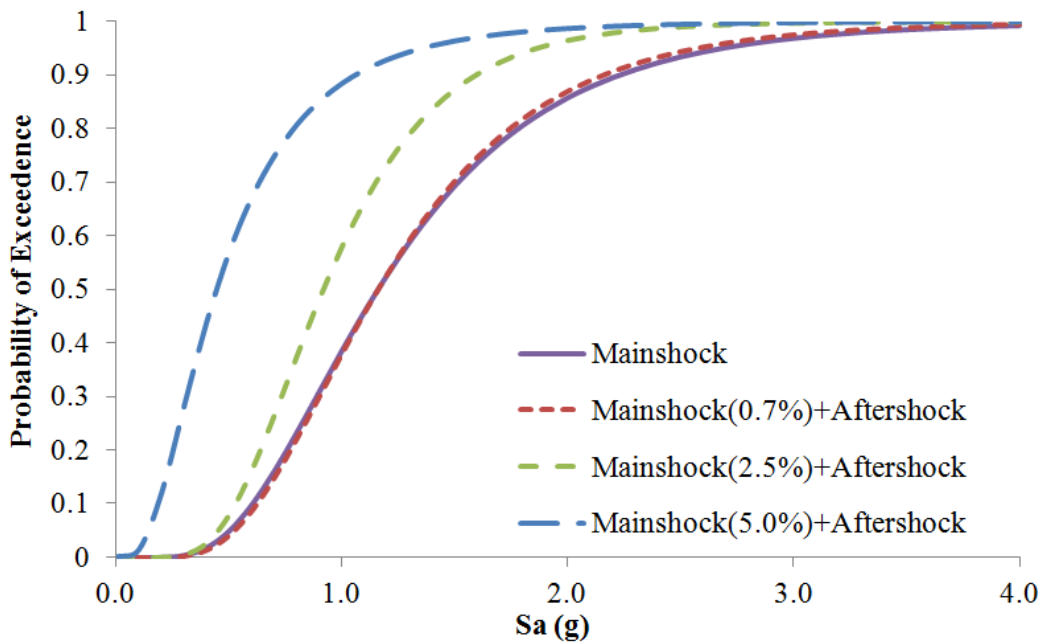
Figure 8. Collapse fragility curve for steel structure after mainshock

The median and logarithmic standards deviation of the collapse damage state threshold for different structural performance levels are listed in Table 3. It reveals that the median value of structural collapse capacity of undamage building is virtlly the same as that of the minorly damage building. The median capacity decreases from 1.16g to 0.92g, a loss of 20% collapse capacity when the building is sujected to a moderate level of earthquake. In comparision, only 1/3 of the original structural collapse capacity remains (i.e., from 1.16g to 0.44g) when severe damage presents in the building. The analysis shows that the structural collapse capacity may reduce significantly if the building is subjected to high intensity mainshock. As a result, the probability of structural collapse increases even if aftershocks with low intensity level are followedafter the mainshock.

Table 3. The statistic of collapse capacity for different structural performance levels

Damage level sustained from mainshock	Median collapse capacity in terms of S_a (g)	logarithmic standards deviation of collapse capacity
N/A	1.16	0.51
Minor	1.16	0.48
moderate	0.92	0.43
severe	0.44	0.68

6. CONCLUSIONS

To promote disaster-resilient communities, building design and construction practices should address the overall risk from earthquakes. Undamaged fragilities and conditional (damaged) fragilities can be combined with aftershock hazard models to quantify the effect of including aftershock seismic hazard in PBE. A better understanding of building performance under mainshock – aftershock sequences will facilitate achieving the objective of PBE, i.e., design strategies and risk levels are consistent with occupant expectations and social objectives.

In order to examine the effects of different structural damage states from mainshock and the following aftershocks on the structural collapse capacity, the scaling rule is provided to combine the mainshock and aftershock. The structural collapse capacity may have a significant reduction when the building is subjected to high intensity mainshock and the structure tends to collapse even if a small aftershock followed by the mainshock. Another way to investigate the effect of aftershocks is to calculate the statistical distribution of Ψ as a function of the aftershock intensity, c.

REFERENCES

Alliard, P-M and Leger, P. (2008) "Earthquake Safety Evaluation of Gravity Dams Considering Aftershocks and Reduced Drainage Efficiency," *Journal of Engineering Mechanics*, **134(1):** 12-22,

ASCE/SEI (2006) Seismic Rehabilitation of Existing Buildings, Report No. **41**, American Society of Civil Engineers,

ATC (2009) Quantification of building seismic performance factors, Report No. **P695**, Federal Emergency Management Agency, Washington, D.C.

Ibarra, L. and Krawinkler, H. (2005) Global Collapse of Frame Structures under Seismic Excitations, Technical report 2005/06, Pacific Earthquake Engineering Research Center (PEER).

Lignos DG, Krawinkler H(2009). Sidesway collapse of deteriorating structural systems under seismic excitations. Report No. TR **172**, The John A. Blume Earthquake Engineering Center, Department of Civil and Environmental Engineering, Stanford University.

Lignos DG. (2008) Prediction and validation of sidesway collapse of two scale models of a 4-story steel moment frame. *Earthquake Engineering and Structural Dynamics*, **40:** 807–825.

Lignos DG, Krawinkler H, Whittaker A. (2011) Prediction and validation of sidesway collapse of two scale models of a 4-story steel moment frame. *Earthquake Engineering and Structural Dynamics*, **40:** 807–825.

OpenSees (2012) The Open System for Earthquake Engineering Simulation http://opensees.berkeley.edu Pacific Earthquake Engineering Research Center (PEER).

Reasenberg, P. A. and Jones, L. M. (1994) "Earthquake aftershocks: update". *Science*, **265(5176):**1251–1252.

RMS. (2008) Reconnaissance Report: The 2008 Wenchuan Earthquake: Risk Management Lessons and Implications, Risk Management Solutions (RMS).

Yeo, G. L. and Cornell, C. A. (2005) "Stochastic characterization and decision bases under time-dependent aftershock risk in performance-based earthquake engineering. Technical report 2005/13, Pacific Earthquake Engineering Research Center (PEER).

Wen, R., Zhou, Z., and Li, X. (2009) "The strong ground motion observation for the Wenchuan aftershock," *Earthquake Science*. **22(2):**181-187.

Vamvatsikos D, Cornell AC.(2002) Incremental dynamic analysis. *Earthquake Engineering and Structural Dynamics,* **31(3):** 491–514.